Geol. Mag. **130** (4), *1993, pp. 443–452.*

Carbon isotope and magnetic polarity evidence for non-depositional events within the Cambrian–Ordovician Boundary section near Dayangcha, Jilin Province, China

R. L. RIPPERDAN*, M. MAGARITZ* & J. L. KIRSCHVINK†

* Department of Environmental Science and Energy Research, Weizmann Institute of Science, Rehovot 76-100, Israel
† Division of Geological and Planetary Sciences, California Institute of Technology, Pasadena, California 91125, U.S.A.

(*Received* 4 August 1992; *accepted* 11 February 1993)

Abstract – Carbon isotope and magnetic polarity stratigraphic results from the Cambrian–Ordovician Boundary section at Xiaoyangqiao, near Dayangcha, Jilin Province, China, in comparison to a contemporaneous section at Black Mountain, Australia, indicate strata equivalent to major portions of the Australian sequence are either absent or are restricted to highly condensed intervals. These intervals are correlative with regressive sea level events identified in Australia and western North America, suggesting regional or eustatic sea level changes strongly influenced deposition of the Xiaoyangqiao sequence. These results also suggest the Xiaoyangqiao section is unfavourable as the site of the Cambrian–Ordovician Boundary Global Stratotype Section and Point.

1. Introduction

Definition of a Global Stratotype Section and Point (GSSP) for the Cambrian–Ordovician Boundary by an International Commission on Stratigraphy Working Group has been hampered in part by concerns about the stratigraphic completeness of the Xiaoyangqiao Critical Section, near Dayangcha, Jilin Province, China. Objections have been voiced because of disagreements over the stratigraphic level for the first appearance datum (FAD) of the conodont species *Cordylodus lindstromi*, a level favoured because of its proximity to the first influx of nematophorous graptolites and widespread occurrence in continental platform and slope facies, and because of the presence of conglomeratic units near the FAD of *C. lindstromi*, raising concerns that hiatuses may exist within the candidate section. Although problems in determining a precise FAD for *C. lindstromi* arising from taxonomic uncertainty have largely been redressed (Nicoll, 1990, 1991, 1992), determination of the stratigraphic completeness of the section continues to be a source of difficulty because of the limitations of biostratigraphic techniques for resolving such problems.

Simultaneous correlation of carbon isotope and geomagnetic polarity reversals provides a correlation framework that can be used independently to refine fossil-based temporal correlations and to assess more accurately stratigraphic completeness. The polarity of the geomagnetic field has the same value simultaneously over the entire Earth's surface, except during geologically very brief periods (< 10 ka) of polarity reversal (Harrison & Somayajulu, 1966; Opdyke, Kent & Lowrie, 1973; others), allowing polarity zonations within different depositional environments to be correlated in 'real time' with high accuracy when properly constrained by other stratigraphic methods. Also, magnetic polarity is a property of the Earth's deep interior and is therefore not sensitive to sedimentary or environmental changes at the surface. Variations in marine inorganic carbon isotopic ratios are found throughout the geological record (Wadleigh & Veizer, 1992; many others), and provide a means for overcoming the non-uniqueness imposed by the binary nature of the polarity reversal record. Major shifts in carbon rations take place rapidly and seem to have global significance (e.g. Zachos & Arthur, 1986; Margolis *et al.* 1987; Magaritz, 1989). Local changes in $\delta^{13}C$ appear to reflect accurately changes in global $\delta^{13}C$ because of the very rapid oceanic mixing rate of carbon dioxide (Holland, 1978; Kump & Garrels 1986), making $\delta^{13}C$ variation a useful stratigraphic marker despite differences in the absolute value of local $\delta^{13}C$. Also, $\delta^{13}C$ values are relatively insensitive to many post-depositional processes because of the extremely low abundance of carbon in pore solutions relative to carbonate rock (Magaritz, 1983; Banner & Hanson, 1990).

We present here new carbon isotope results from the GSSP-candidate Cambrian–Ordovician boundary section at Xiaoyangqiao, China. These results, in combination with existing magnetic polarity data (R. L. Ripperdan, unpub. Ph.D. thesis, Cal. Inst. Tech., 1990) and biostratigraphic information (Chen *et al.* 1988), have been used to assess the stratigraphic continuity of the section. The simultaneous occurrences of polarity reversals, sharp changes in the $\delta^{13}C$ profile, and biostratigraphic boundaries within the Xiaoyangqiao section strongly suggest underlying

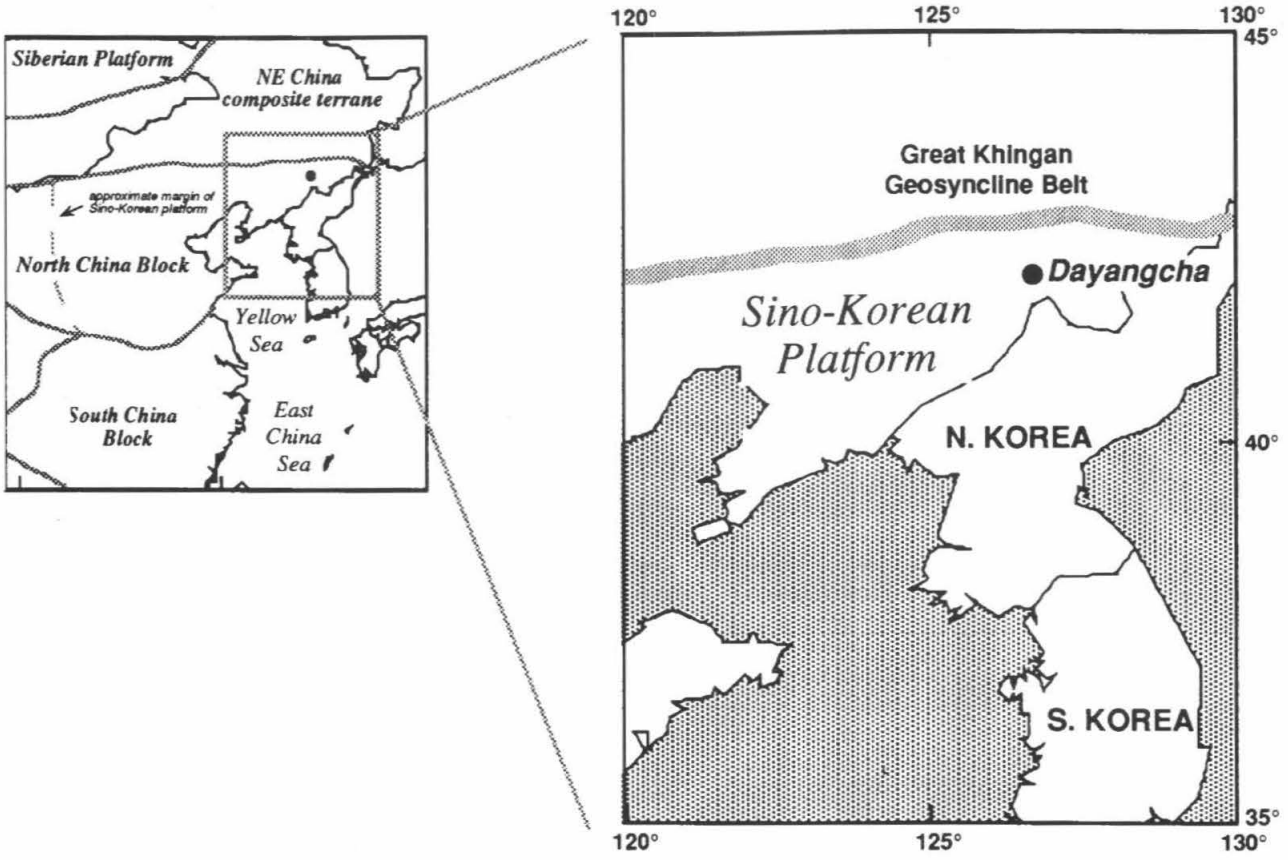

Figure 1. Generalized location map for the Dayangcha area, northeast China. (See Chen *et al.* 1988 for detailed index maps.)

hiatuses or intervals of extremely low depositional rates. We then correlate these results to those from the contemporaneous section at Black Mountain, western Queensland, Australia, and show that these intervals correlate to previously identified regressive sea level events within the Australian sequence and in the western United States.

2. Geologic setting

The sections at Xiaoyangqiao, near Dayangcha, in Jilin province, northeastern China, have become internationally prominent from their status as a candidate for placement of the Cambrian–Ordovician boundary Global Stratotype Section and Point (GSSP). The Xiaoyangqiao Critical Section (XCS) is the middle of three overlapping segments spanning the *Proconodontus tenuiserratus* to *Cordylodus angulatus* zones (~ 10 Ma; Harland *et al.* 1990), and contains the base of the *Cordylodus lindstromi* Zone, the level currently most favoured for placement of the boundary GSSP.

The sections lie within the Changbaishan Mountains near the northern margin of the Sino-Korean Platform (Fig. 1). They consist of rhythmical fine-grained carbonates, with intermittent clastic deposits superimposed upon the primary periodic sequence, and were deposited in moderately deep water along the outer shelf of the platform (Chen *et al.* 1988). Exposures are found in steep stream banks, are relatively fresh, and dip uniformly 30° to the south–southeast with no obvious faulting or folding. A conodont alteration index value of 1.5 (Chen *et al.* 1988) suggests the area has not been subjected to appreciable thermal metamorphism or been deeply buried (Epstein, Epstein & Harris, 1977).

Detailed biostratigraphic zonations have been established for conodonts and trilobites, and a number of other groups have been studied, including graptolites and acritarchs (see Chen *et al.* 1986; Chen *et al.* 1988). The occurrence of nematophorous graptolites immediately above the appearance of *Cordylodus lindstromi* has been a primary factor for continued consideration of the section as the Cambrian–Ordovician GSSP.

3. Results

One hundred and thirty core samples were collected from the Xiaoyangqiao Critical and Upper Sections in conjunction with a visit by the International Working Group on the Cambrian–Ordovician Boundary in August, 1986. Sampling intervals were less than one metre for most of the section and were tightly

constrained to the local lithostratigraphy and previous sampling traverses. Sampling details are given in Table 1.

Carbonate whole rock isotopic analyses were performing using the conventional phosphoric acid method for generating CO_2 gas (McCrea, 1950). Samples were measured on a Varian MAT250 gas ionization mass spectrometer; the results are listed in Table 1. Reproducibilities were better than 0.1‰ for $\delta^{13}C$ and 0.2‰ $\delta^{18}O$. Results were determined using standards calibrated against NBS-19 ($\delta^{13}C = +1.92‰$, $\delta^{18}O = -2.20‰$ vs. Peedee Belemnite; Coplen, Kendall & Hopple, 1983). Standard dissolution times were 24 h at 28 °C for samples with < 10 mol% dolomite, and 48 h for all others. A single sample containing > 40 mol% dolomite was evacuated after 4 h dissolution to remove CO_2 generated from the calcite fraction. Dolomite/total carbonate values were determined by X-ray diffraction after the method of Füchtbauer & Goldschmidt (1965).

Carbon and oxygen isotope profiles from carbonate rocks are shown in Figure 2. $\delta^{13}C$ values ranged between −0.3‰ and +1.3‰ (vs. PDB). The $\delta^{13}C$ profile is marked by a sharp 0.7% rise at the base of Bed 8, followed by a 1.5‰ drop through the next 15 m, culminating at the base of Bed 13. $\delta^{13}C$ values show a small positive cycle between −0.2‰ and +0.3‰ throughout Bed 13 and Bed 14 (5 m), and then rise sharply by about 0.7‰ at the base of Bed 16, followed by an interval of fairly stable $\delta^{13}C$ with a broad lowering of $\delta^{13}C$ near the base of the *Cordylodus angulatus* Zone.

Oxygen isotope values ranged between $\delta^{18}O = -11‰$ and −8‰ (vs. PDB). Although long-ranging trends in the $\delta^{18}O$ profile were similar to those seen in $\delta^{13}C$, changes in $\delta^{18}O$ were not directly correlative with $\delta^{13}C$ (Fig. 3) at the sample level, except for a tendency towards lower $\delta^{18}O$ and $\delta^{13}C$ values in mudstones and shales. The $\delta^{18}O$ values are consistent with those from other Palaeozoic carbonate rocks (Wadleigh & Veizer, 1992), and probably reflect exchange with meteoric or diagenetic fluids during shallow burial conditions (see Banner & Hanson, 1990) rather than depositional values. Inferred temperatures based on the conodont alteration index noted above are compatible with this mechanism.

4. Discussion

The Black Mountain section in western Queensland, Australia provides an excellent basis for comparison of the Xiaoyangqiao results. The two sections were probably separated by no more than 1000 m at the end of the Cambrian (Burrett & Stait, 1986; Scotese, 1987; Burrett, Long & Stait, 1990; Kirschvink, 1992; Ripperdan & Kirschvink, unpub. data). Deposition during the boundary interval was apparently continuous at Black Mountain (Druce, Shergold & Radke, 1982), and detailed conodont, palaeomagnetic, and carbon isotope stratigraphies have been recently described (Nicoll & Shergold, 1991; Shergold & Nicoll, 1992; Ripperdan & Kirschvink, 1992; Ripperdan *et al.* 1992).

Both sections display a rapid rise in $\delta^{13}C$ near the FAD of *Cordylodus proavus*, followed by a rapid lowering of $\delta^{13}C$ to a minimum at the base of the *H. simplex* Zone (≈ *Cordylodus intermedius* Zone) (Fig. 4). An overlying 1.5‰ positive $\delta^{13}C$ cycle spans the 100 m-thick *H. simplex* Zone at Black Mountain, whereas a smaller, poorly defined positive $\delta^{13}C$ cycle encompassing the entire *C. intermedius* Zone occurs within only a 5 m interval in the Xiaoyangqiao section. Both profiles show subsequent sharp rises from these levels, with $\delta^{13}C$ values stabilizing and then broadly declining towards the base of the *Cordylodus angulatus* Zone.

Despite their similarities, the sections have important differences at two key levels: within the lower *Cordylodus proavus* Zone, and within the lower *Cordylodus lindstromi* Zone. These differences are outlined below.

4.a. Lower *Cordylodus proavus* Zone

At Xiaoyangqiao, a discontinuity in the $\delta^{13}C$ profile occurs within Bed 8 between samples XCS 40 and XCS 41 (Fig. 2). XCS 40 was taken from the same level as the first appearance datum (FAD) of *Fryxellodontus inornatus*. At Black Mountain, the lowest *F. inornatus* as found 35 metres below the maximum $\delta^{13}C$ values within the *Cordylodus proavus* Zone (Fig. 4); at Xiaoyangqiao, the interval between the FAD of *F. inornatus* and maximum $\delta^{13}C$ is less than 0.5 metres within Bed 8.

Underlying strata with normal polarity at Xiaoyangqiao can be correlated to the F1+ normal polarity magnetozone within the upper *Hispidodontus appressus* Zone at Black Mountain. This alternative is favoured by comparisons with the last occurrence datum (LOD) of *Proconodontus muelleri*. At Black Mountain, the LOD of *P. muelleri* is above the top of the F1+ interval; at Xiaoyangqiao, the LOD of *P. muelleri* is in Bed 5, within the upper part of the F+ interval (Chen *et al.* 1986, table 16, p. 102). Since the range of *P. muelleri* typically does not overlap the range of *Fryxellodontus inornatus* (Miller, 1988), and the F3+ magnetozone at Black Mountain is at the FAD of *F. inornatus*, it is unlikely that the F3+ magnetozone is correlative with the bulk of the F+ zone at Xiaoyangqiao. It is possible that the Bed 7 portion of the F+ magnetozone at Xiaoyangqiao is correlative to the F3+ magnetozone at Black Mountain, with strata equivalent to the intervening F2− zone absent, but the lack of supporting $\delta^{13}C$ data and a 1.7 m gap in the magnetic polarity profile make this only a speculative suggestion.

Table 1. Sampling numbers, stratigraphic positions, carbon and oxygen isotope data, magnetic polarity interpretation, positions with respect to previous sampling traverses and important stratigraphic horizons

Sample	HT (m)	$\delta^{13}C$	$\delta^{18}O$	Polarity	Location	Notes
XCS 2	0.4	0.51	−9.67	—	0.1 m above 1-A	
XCS 6	1.4	0.30	−9.54	—	at 1-C_1	
XCS 7	1.5	0.31	−9.55	normal	at 1-C_2	
XCS 11	2.8	0.64	−8.81	—	—	
XCS 12	3.0	0.58	−8.80	—	—	
XCS 13	3.1	0.04	−9.87	—	at 1-E	
XCS 13A	3.4	0.52	−8.99	—	0.1 m below 2-A	
XCS 14	4.4	0.48	−9.46	normal	at 2-B	
XCS 15	4.6	—	—	reversed	at 2-D	
XCS 16	4.6	0.69	−8.93	normal	at 2-E	
XCS 17	5.4	—	—	normal	at 2-H	
XCS 18	5.6	0.40	−9.16	normal	—	
XCS 19	5.8	0.57	−8.99	normal	0.1 m above 2-I	
XCS 20	5.9	—	—	normal	—	
XCS 21	6.3	—	—	normal	—	
XCS 22	6.4	—	—	normal	at 3–2	
XCS 23	6.6	0.44	−8.84	normal	midway 3–3, 3–4	
XCS 24	6.8	0.24	−8.87	—	at 3-A_1	
XCS 25	6.9	0.62	−9.17	normal	at 3-A_2	
XCS 26	7.3	0.50	−9.15	normal	at 3-C_1	
XCS 27	7.3	0.66	−8.86	—	at 3-C_2	
XCS 28	7.4	0.53	−9.28	—	—	
XCS 29	7.9	0.62	−9.56	normal	at 3-E	
XCS 30	8.3	0.39	−9.68	—	at 3-E	
XCS 31	8.3	0.26	−9.13	—	0.1 m below 3-F	
XCS 32	8.6	0.52	−9.16	—	at 3-G	
XCS 33	8.9	0.11	−9.23	—	0.1 m above 5	LOD *Proconodontus muelleri*
XCS 36	9.6	—	—	normal	—	
XCS 38	10.7	0.73	−8.86	normal	0.1 m below 7-B	Above FAD *Cordylodus proavus*
XCS 39	11.4	0.72	−8.88	normal	at top of 7-B	
XCS 40	11.7	0.52	−8.44	—	at 8-A	FAD *Fryxellodontus inornatus*
XCS 41	12.2	1.25	−8.70	—	0.2 m below 8-C	
XCS 42	12.6	1.30	−8.55	—	0.2 m above 8-C	
XCS 43	13.0	—	—	—	at top of 8-D	
XCS 44	13.3	1.29	−8.28	—	—	
XCS 45	15.0	1.42	−7.69	—	near 9-4	
XCS 47	15.8	0.80	−9.32	—	at 9-5	
XCS 48	16.0	1.14	−8.64	—	at 9-6	
XCS 49	16.6	1.11	−8.58	reversed	0.1 below 9-8	
XCS 50	16.9	1.16	−8.35	—	0.1 above 9-9	
XCS 51	17.3	0.97	−8.76	—	at 9-11	
XCS 52	17.6	0.89	−8.47	reversed	—	
XCS 53	17.9	0.96	−8.31	—	—	
XCS 54	18.4	0.85	−8.71	reversed	at 9-12	
XCS 55	18.8	1.05	−8.84	reversed	at 9-13	
XCS 56	19.4	0.62	−8.89	reversed	at 9-A_2	
XCS 57	20.0	0.77	−8.74	reversed	at 9-A_4	
XCS 58	20.5	0.75	−8.89	reversed	at 9-B_2	
XCS 59	20.9	0.71	−8.69	reversed	at 9-C_2	
XCS 60	22.0	0.71	−8.65	—	at 9-D_2	
XCS 61	23.2	—	—	reversed	0.1 m below 9-E_2	
XCS 62	23.8	—	—	reversed	—	
XCS 63	24.5	0.33	−8.78	reversed	midway 10-3, 10-4	
XCS 64	25.2	0.29	−9.01	—	at 10-5	
XCS 65	25.7	−0.12	−9.88	reversed	—	
XCS 68	27.2	−0.08	−10.23	reversed	—	
XCS 70	27.7	−0.06	−9.09	reversed	at 10-A_5	
XCS 71	28.0	0.32	−8.71	—	—	
XCS 72	28.8	−0.13	−9.24	—	at 11-AO_2	
XCS 74	29.0	0.24	−9.23	reversed	at 11-A_1	FAD *Cordylodus intermedius; Hirsutodontus simplex*
XCS 75	29.3	0.32	−9.03	—	0.1 m below 11-A_3	
XCS 76	30.5	0.12	−8.35	—	at base of 11-B	
XCS 77	31.1	0.16	−9.81	reversed	at 12-2	
XCS 78	31.7	−0.11	−10.74	reversed	—	
XCS 79	32.3	0.63	−8.50	reversed	in 13-F	Above FAD *Cordylodus lindstromi*
XCS 81	33.2	—	—	reversed	at 13-J	
XCS 82	34.1	—	—	normal	at 13-O	FAD nematophorous graptolites
XCS 83	34.6	0.70	−9.34	normal	at 14-1	
XCS 85	35.4	0.59	−9.45	—	at 15-A	
XCS 86	36.1	0.61	−9.52	—	at 15-D	

Table 1. (*cont.*)

Sample	HT (m)	$\delta^{13}C$	$\delta^{18}O$	Polarity	Location	Notes
XCS 87	36.5	—	—	normal	at 16-2	
XCS 88	36.9	0.34	−10.02	normal	in 17-A	
XCS 89	37.2	—	—	normal	—	
XCS 90	37.6	0.36	−10.00	normal	midway 17-D, 17-E	
XCS 91	38.0	0.37	−9.74	—	0.1 m below 17-F	
XCS 92	38.2	0.34	−9.91	—	0.1 m above 17-F	
XCS 93	38.4	0.53	−9.73	—	at 17-G	
XCS 94	38.9	0.55	−9.81	—	at 17-I	
XCS 95	39.7	0.74	−8.50	normal	at 18-C	
XCS 96	—	—	—	normal	—	
XCS 97	40.3	0.52	−10.13	normal	0.1 m above 20	
XCS 98	40.5	0.57	−9.63	normal	at 21	
XCS 99	41.0	0.69	−8.36	normal	at 22-F	
XCS 100	41.2	0.39	−10.22	normal	at 22-G	
XCS 101	41.6	0.74	−9.13	normal	0.2 m above 23-B	
XCS 102	44.5	0.71	−8.80	normal	0.2 m above 25-G	
XCS 103	44.8	0.38	−9.66	normal	0.2 m below 25-H	
XCS 104	44.9	0.51	−8.82	normal	0.3 m above 26-A	
XCS 105A	48.0	0.53	−8.93	—	—	
XUS 106	49.0	0.70	−9.46	normal	—	
XUS 107	49.4	0.95	−9.20	—	at 28-1	
XUS 108	49.8	0.76	−8.09	—	at 28-3	
XUS 109	50.2	0.75	−7.99	—	at 28-4	
XUS 110	51.4	0.62	−8.22	normal	at 28-7	
XUS 111	52.0	0.59	−8.37	normal	at $29\text{-}1_2$	
XUS 112	53.0	0.44	−8.37	normal	at $29\text{-}1_4$	
XUS 113	53.0	0.49	−8.37	normal	—	
XUS 114	54.3	0.39	−8.30	—	midway 29-2, 29-3	FAD *Cordylodus angulatus*
XUS 115	55.9	0.24	−8.76	—	at 29-4	
XUS 117	58.1	0.26	−8.34	—	—	
XUS 118	60.4	0.02	−8.53	—	in 29-7	
XUS 119	62.0	0.26	−8.13	—	in 30-1	
XUS 120	65.2	0.38	−8.27	—	—	
XUS 121	66.5	−0.12	−8.54	—	—	
XUS 122	69.6	0.38	−8.19	normal	in 30-3	
XUS 123	71.3	0.18	−8.55	—	in 30-4	
XUS 124	73.3	0.11	−8.48	normal	—	
XUS 125	75.3	0.07	−8.29	—	in 31-1.5	FAD *Chosonodina herfurthi*
XUS 126	78.4	0.14	−8.24	—	in 31-2.5	
XUS 127	81.6	−8.08	−8.56	reversed	in 31-4.5	
XUS 128	83.4	—	—	normal	—	

XCS – Xiaoyangqiao Critical Section; XUS – Xiaoyangqiao Upper Section. Locations are based on HDA sampling numbers given in Chen *et al.* (1986, 1988).

An alternative correlation would place the lower 12 m at Xiaoyangqiao entirely within the F3+ magnetozone, but this possibility is less favoured because (a) the F3+ magnetozone occurs within only one sample at Black Mountain, while the F+ magnetozone ranges through 16 at Xiaoyangqiao; (b) $\delta^{13}C$ values at the F3+ level at Black Mountain are only 0.3‰ lower than the maximum value, while at Xiaoyangqiao the $\delta^{13}C$ value of the underlying strata averages ~ 0.7‰ lower than the maximum; and (c) the required overlapping of the ranges of *Fryxellodontus inornatus*, *Cambrooistodus cambricus*, and *Proconodontus muelleri* is incompatible with current understanding of North American conodont faunas through the boundary interval (Miller, 1988).

Based on the first correlation, the approximately 70 m of section found at Black Mountain between the top of the F1+ magnetozone and the *C. proavus* Zone $\delta^{13}C$ maximum are represented by no more than 1.5 m of section at Xiaoyangqiao. If the speculative correlation of the F3+ interval to Bed 7 is correct, then virtually all of the *Hispidodontus discretus* Zone at Black Mountain is absent from the Xiaoyangqiao section, or is restricted to a 1.7 m interval from which palaeomagnetic information was not obtained. In the unlikely event that the alternative correlation is correct, then deposition would have been relatively undisrupted through the lower 12 m of the Xiaoyangqiao section.

Depositional breaks or condensed intervals near Beds 7 and 8 at Xiaoyangqiao may be directly correlated to stages of the Lange Ranch Eustatic Event, identified at various localities across the western United States, Australia, and North China (Miller, 1984, 1992; Nicoll *et al.* 1992).

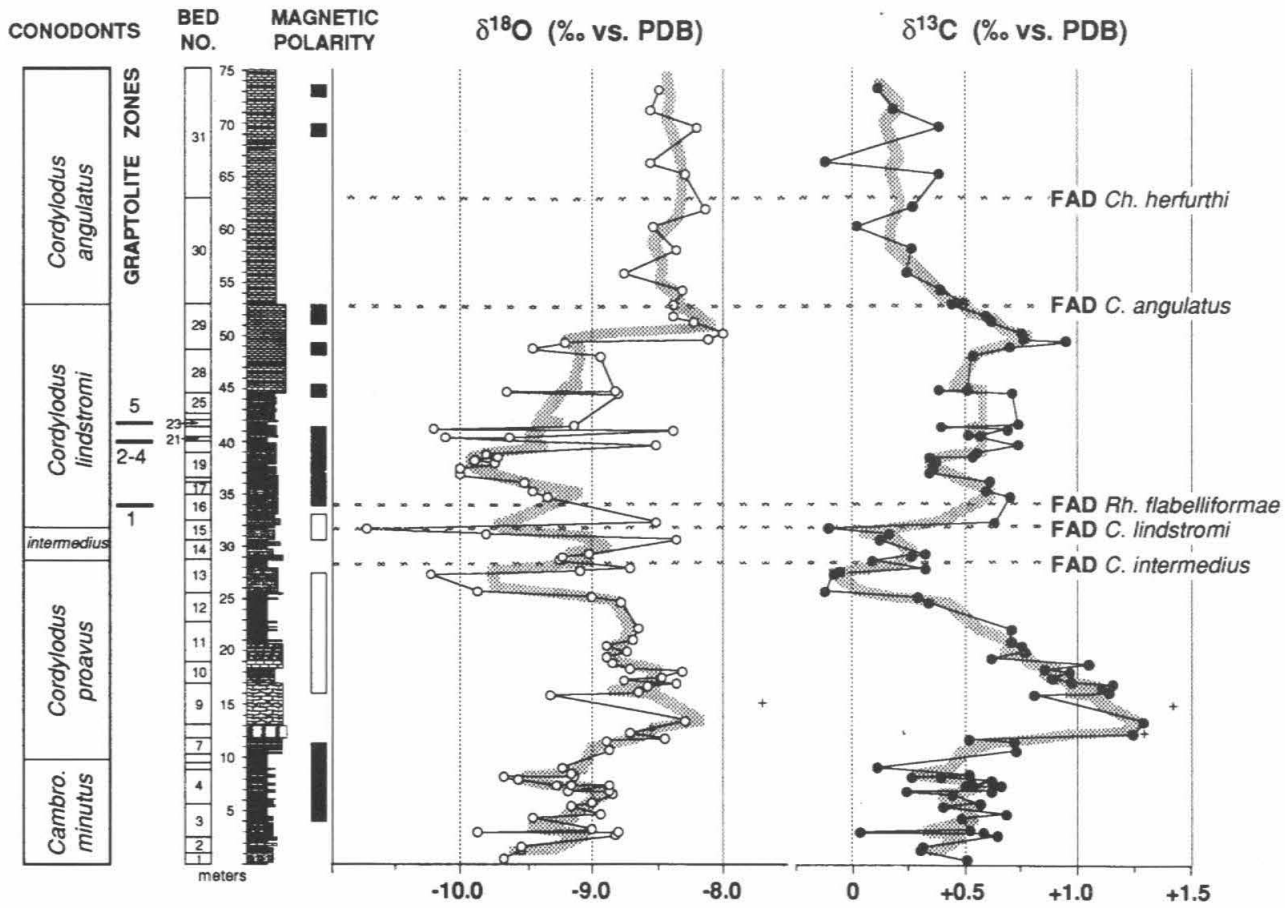

Figure 2. Carbon and oxygen isotope profiles from the Xiaoyangqiao Critical and Upper Sections (XCS, XUS) near Dayangcha. Lithostratigraphy and biostratigraphy from Chen *et al.* 1986, 1988); magnetic polarity profile from R. L. Ripperdan, unpub. Ph.D. thesis, Cal. Inst. Tech., 1990. FAD = first appearance datum. Plus symbols in both profiles represent samples with > 20 mol% dolomite. The thick-shaped isotope profiles represent smoothing of all data by moving average (period = 3), which minimizes non-systematic variability.

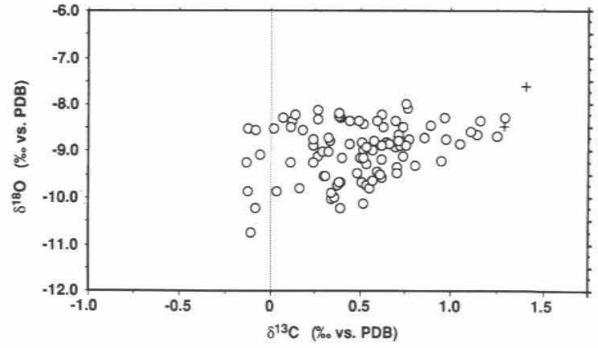

Figure 3. $\delta^{18}O$ vs. $\delta^{13}C$ from carbonate rocks at Xiaoyangqiao. Plus symbols represent samples with > 20 mol% dolomite.

4.b. Lower *Cordylodus lindstromi* Zone

The first evidence of a magnetic polarity reversal at this level at Xiaoyangqiao was found at the same sampling horizon as the first appearance of nematophorous graptolites, in sample HDA 13-O of Bed 16 (sample XCS 82). Sampling resolution in this part of the section was high, and the polarity change is thus constrained to lie within 0.9 m of XCS 82. The proximity of these two independent marker events raises suspicions that their superposition may be due to an underlying hiatus or a condensed interval.

Based on the conodont biostratigraphy, the polarity reversal at this level can be confidently correlated to the H+ magnetozone at Black Mountain. Equating the base of magnetozone H+ to sample XCS 82 requires that the lower 50 m of the Black Mountain *Cordylodus lindstromi* Zone be represented by only 2–3 m at Xiaoyangqiao. Furthermore, the highest $\delta^{13}C$ values above the *Cordylodus proavus* Zone at Xiaoyangqiao do not approach the value of the maximum within that zone until well up into the *C. lindstromi* Zone; while at Black Mountain, $\delta^{13}C$ maxima within the *Cordylodus prolindstromi* and *Hirsutodontus simplex* zones are virtually identical to that in the *C. proavus* Zone. This suggests that the *H. simplex* and *C. prolindstromi* zones may be poorly represented within the Xiaoyangqiao section, which is compatible with observations by some participants in the 1986 field excursion that Beds 14 and 15 are primarily turbidites and debris flows (J. Repetski, R.

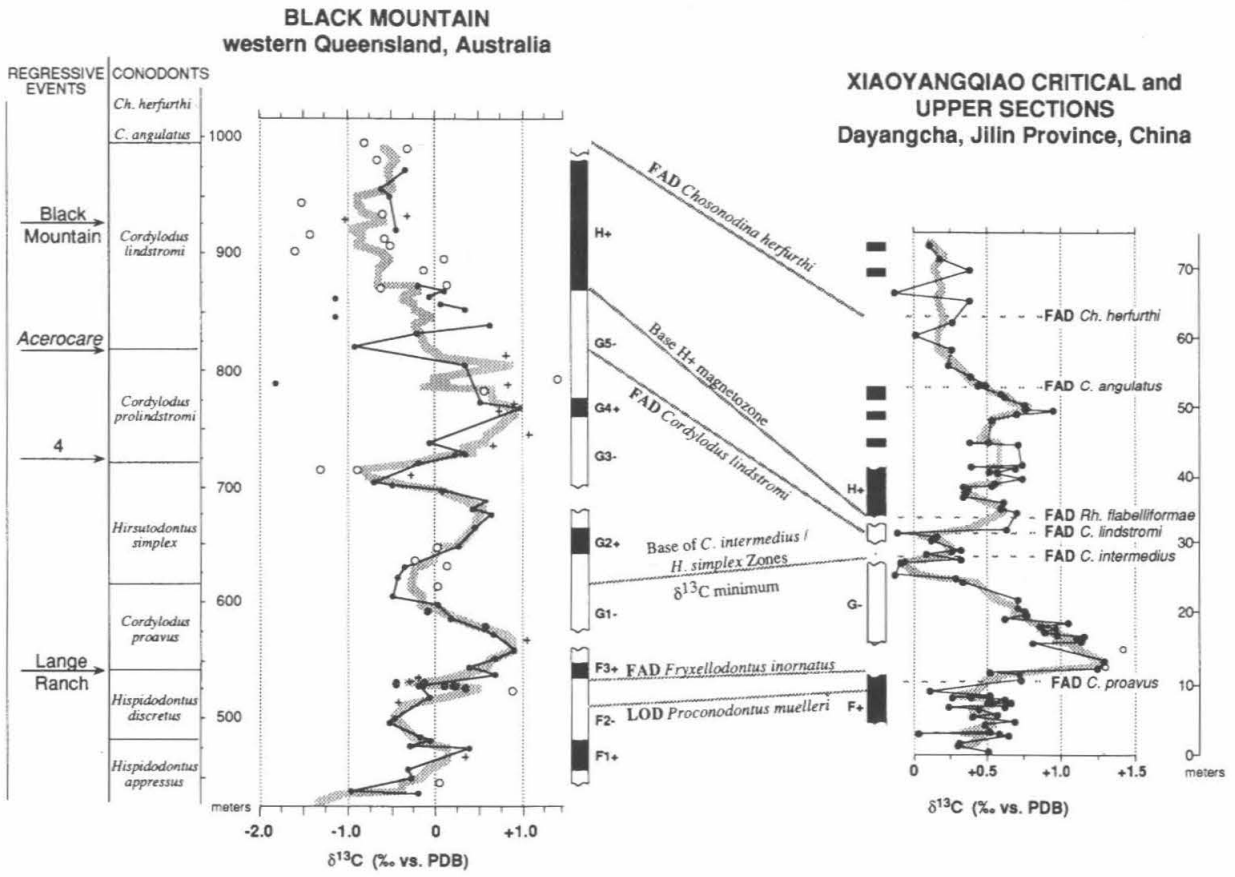

Figure 4. Correlation of $\delta^{13}C$ and magnetic polarity profiles between Black Mountain, Australia (left) and Xiaoyangqiao. Black Mountain magnetic polarity results from Ripperdan & Kirschvink (1992); carbon isotope results from Ripperdan *et al.* (1992). Biostratigraphy modified from Shergold & Nicoll (1992) to accommodate stratigraphic positions of Ripperdan & Kirschvink (1992); assemblage zone boundaries relative to sampling profile are precise. Regressive events from Nicoll *et al.* (1992) have been similarly modified.

Ethington, and M. Taylor, International Working Group on the Cambrian–Ordovician Boundary Circular 27, Appendix 3). Current investigations by M. Linström should further understanding of the sedimentology in this critical interval.

4.c. Interpretations

Our interpretation of the depositional history of the Xiaoyangqiao Critical and Upper sections is given in Fig. 5. The primary constraint used in constructing this diagram was that the correlation tie-lines used in Figure 4 be made parallel, or nearly so. This method highlights differential variations in depositional rates. It was assumed for purposes of comparison that the Black Mountain sequence preserves a continuous record of the Cambrian–Ordovician Boundary interval.

Deposition in the lower part of the Xiaoyangqiao Critical Section may have been disrupted at least twice, near Beds 5 to 7 and within Bed 8, by both stages of the Lange Ranch Eustatic Event (LREE) (Miller, 1984, 1992; Nicoll *et al.* 1992). Based on the FAD of *Cordylodus proavus*, we interpret the F3+ magnetozone to be present in Bed 7, indicating that the entire F2− magnetozone is absent from the Xiaoyangqiao section. A depositional break at this level is consistent with evidence from other localities for the first stage of the LREE. Another disruption is interpreted to occur within the lower part of Bed 8, immediately above the FAD of *Fryxellodontus inornatus*, and may be represented by a highly condensed interval rather than actual hiatus. In the western United States and at Wushan, North China, the FAD of *F. inornatus* is coincident with or immediately below shallowing-upwards sequences and disconformities marking the second regressive stage of the Lange Ranch Eustatic Event (Miller, 1984, 1992).

Deposition appears to have been nearly continuous through the upper portions of the *Cordylodus proavus* Zone. A steady decline in $\delta^{13}C$ values is present in both sections, culminating at the base of the *Hirsutodontus simplex* and *Cordylodus intermedius* Zones.

A major change in deposition is suggested between Beds 13 and 16. The positive $\delta^{13}C$ cycle found within the *Hirsutodontus simplex* Zone at Black Mountain, and the more poorly-defined interval of higher $\delta^{13}C$ within the *Cordylodus prolindstromi* Zone, appear to have no firm correlatives within the Xiaoyangqiao section. The interval immediately above the FAD of

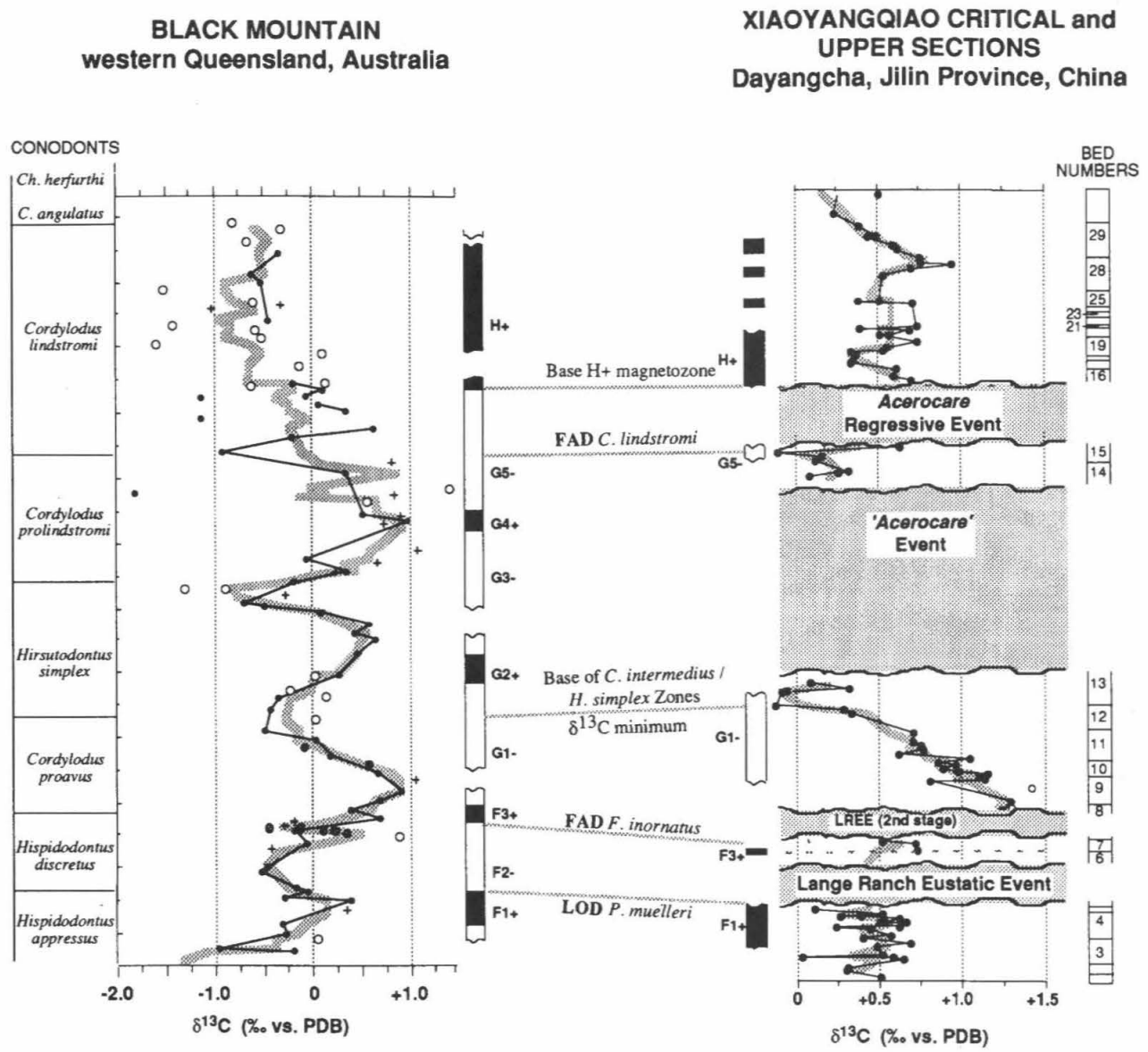

Figure 5. Interpretative diagram for the depositional history of the Xiaoyangqiao Critical Section. *Acerocare* Regressive Event *sensu* Nicoll *et al.* (1992); '*Acerocare*' Event *sensu* Erdtmann (1986) (see text for discussion).

Cordylodus lindstromi may be directly correlatable to the *Acerocare* Regressive Event as defined in Australia (Nicoll *et al.* 1992). We interpret the extended interval of apparent non-deposition or condensation immediately below the base of the *Cordylodus lindstromi* Zone as correlative to the '*Acerocare* Event' of Erdtmann (1986), which refers to a more prolonged period of sea level oscillations occurring throughout the *Acerocare* Zone in Scandinavia.

5. Conclusions

Correlations based on carbon isotope and magnetic polarity profiles from the Cambrian–Ordovician boundary section at Xiaoyangqiao, near Dayangcha, Jilin Province, China, and the contemporaneous section at Black Mountain, Australia indicate that at least two prominent periods of non-deposition or extremely slow deposition occurred during accumulation of the Xiaoyangqiao sequence. These can be correlated to regressive events identified in Australia, western North America, and Scandinavia, suggesting that sea level change strongly influenced deposition of the Xiaoyangqiao sequence. Despite the uncertain status of the first appearance datum of *Cordylodus lindstromi*, these major depositional breaks or condensed intervals occur very close to the proposed horizon for placement of the boundary GSSP. This suggests that the Xiaoyangqiao section may be unsuitable as a GSSP for the Cambrian–Ordovician boundary.

Acknowledgements. The authors wish to thank the Organizing Committees for the 1986 meeting of the Cambrian–Ordovician Boundary Working Group in Dayangcha for permission to work in their respective areas, and for their

assistance in collecting samples. Laboratory and sampling assistance by A. Kobayashi-Kirschvink and R. Selnikov are gratefully acknowledged. J. L. Miller and two anonymous reviewers contributed helpful comments to improve this paper. This work was supported by NSF Grants EAR-8721391 and PYI-8351370, by contributions from the Chevron Oil Field Research Company and the Arco Foundation, and by a Sir Charles Clore postdoctoral fellowship to the senior author. Weizmann Institute of Science Department of Environmental Science and Energy Research contribution 66; CIT Division of Geological and Planetary Sciences contribution 5176.

References

BANNER, J. L. & HANSON, G. N. 1990. Calculations of simultaneous isotopic and trace element variations during water–rock interaction with applications to carbonate diagenesis. *Geochimica et Cosmochimica Acta* **54**, 3123–37.

BURRETT, C. & STAIT, B. 1986. China and southeast Asia as part of the Tethyan margin of Cambro–Ordovician Gondwanaland. In *Shallow Tethys* 2 (ed. K. G. McKenzie), pp. 65–77. International Symposium on Shallow Tethys 2, Wagga Wagga.

BURRETT, C., LONG, J., & STAIT, B. 1990. Early-Middle Paleozoic biogeography of Asian terranes derived from Gondwana. In *Palaeozoic Palaeogeography and Biogeography* (eds W. S. McKerrow and C. R. Scotese), pp. 163–174. *Geological Society Memoirs* **12**, Bath.

CHEN J.-Y., ERDTMANN, B.-D., GONG W.-L., LI H.-M., LIN Y.-K., QIAN Y.-Y., TAO W.-C., WANG Y.-X., WANG Z.-Z., YANG J.-D., YIN L.-M. & ZHANG J.-M. 1986. *Aspects of Cambrian–Ordovician Boundary in Dayangcha, China*. Beijing: China Prospect Publishing House.

CHEN J.-Y., QIAN Y.-Y., ZHANG J.-M., LIN Y.-K., YIN L.-M., WANG Z.-H., WANG Z.-Z., YANG J.-D. & WANG Y.-X. 1988. The recommended Cambrian–Ordovician boundary stratotype of the Xiaoyangqiao section (Dayangcha, Jilin Province), China. *Geological Magazine* **125**, 415–44.

COPLEN, T. B., KENDALL, C., & HOPPLE, J. 1983. Comparison of stable isotope reference samples. *Nature* **302**, 236–8.

DRUCE, E. C., SHERGOLD, J. H. & RADKE, B. M. 1982. A reassessment of the Cambrian–Ordovician boundary section at Black Mountain, western Queensland, Australia. In *The Cambrian–Ordovician Boundary: Sections, Fossils Distributions, and Correlations* (eds M. G. Bassett and W. T. Dean), pp. 193–209. National Museum of Wales, Geological Series 3, Cardiff.

EPSTEIN, A. G., EPSTEIN, J. B. & HARRIS, L. D. 1977. *Conodont color alteration – an index of organic metamorphism*. U.S. Geological Survey Professional Paper no. 995, 27 pp.

ERDTMANN, B.-D. 1986. Early Ordovician eustatic cycles and their bearing on punctuations in early nematophorid (planktic) graptolite evolution. *Lecture Notes in Earth Sciences* **8**, 139–52.

FÜCHTBAUER, H. & GOLDSCHMIDT, H. 1965. Beziehungen zwischen Calciumgehalt und Bildungsbedingungen der Dolomite. *Geologische Rundschau* **55**, 29–40.

HARLAND, W. B., ARMSTRONG, R. L., COX, A. V., CRAIG, L. E., SMITH, A. G. & SMITH, D. G. 1990. *A Geologic Time Scale*. Cambridge: Cambridge University Press.

HARRISON, C. G. A. & SOMAYAJULU, B. L. K. 1966. Behaviour of the Earth's magnetic field during a reversal. *Nature* **212**, 1193–5.

HOLLAND, H. D. 1978. *The Chemistry of the Atmosphere and Oceans*. New York: John Wiley & Sons.

KIRSCHVINK, J. L. 1992. A paleogeographic model for Vendian and Cambrian time. In *The Proterozoic Biosphere: A Multidisciplinary study* (eds J. W. Schopf, C. Klein and D. Des Maris), pp. 567–81. Cambridge University Press.

KUMP, L. R. & GARRELS, R. M. 1986. Modeling atmospheric O_2 in the global sedimentary redox cycle. *American Journal of Science* **286**, 337–60.

MAGARITZ, M. 1983. Carbon and oxygen isotope composition of recent and ancient coated grains. In *Coated Grains* (ed. T. M. Peryt), pp. 27–37. Berlin: Springer-Verlag.

MAGARITZ, M. 1989. ^{13}C minima follow extinction events: A clue to faunal radiation. *Geology* **17**, 337–40.

MARGOLIS, S. V., MOUNT, J. F., DOEHNE, E., SHOWERS, W. & WARD, P. 1987. The Cretaceous/Tertiary boundary carbon and oxygen isotope stratigraphy, diagenesis, and paleoceanography at Zumaya, Spain. *Paleoceanography* **2**, 361–77.

MCCREA, J. M. 1950. On the isotopic chemistry of carbonate and a paleo-temperature scale. *Journal of Chemical Physics* **18**, 849–57.

MILLER, J. F. 1984. Cambrian and earliest Ordovician conodont evolution, biofacies, and provincialism. In *Conodont Biofacies and Provincialism* (ed. D. L. Clark), pp. 43–68. Geological Society of America Special Paper no 196.

MILLER, J. F. 1988. Conodonts as biostratigraphic tools for redefinition and correlation of the Cambrian–Ordovician boundary. *Geological Magazine* **125**, 349–62.

MILLER, J. F. 1992. The Lange Ranch Eustatic Event: A regressive–transgressive couplet near the base of the Ordovician System. In *Global Perspectives on Ordovician Geology* (eds B. Webby and J. R. Laurie), pp. 395–407. Rotterdam: Balkema.

NICOLL, R. S. 1990. The genus *Cordylodus* and a latest Cambrian–earliest Ordovician conodont biostratigraphy. *Bureau of Mineral Resources Journal of Australian Geology and Geophysics* **11**, 529–58.

NICOLL, R. S. 1991. Differentiation of Late Cambrian–Early Ordovician species of *Cordylodus* (Conodonta) with biapical basal cavities. *Bureau of Mineral Resources Journal of Australian Geology and Geophysics* **12**, 223–44.

NICOLL, R. S. 1992. Evolution of the conodont genus *Cordylodus* and the Cambrian–Ordovician boundary. In *Global Perspectives on Ordovician Geology* (eds B. Webby and J. R. Laurie), pp. 93–103. Rotterdam: Balkema.

NICOLL, R. S. & SHERGOLD, J. H. 1991. Revised Late Cambrian (pre-Payntonian–Datsonian) conodont biostratigraphy at Black Mountain, Georgina Basin, western Queensland, Australia. *Bureau of Mineral Resources Journal of Australian Geology and Geophysics* **12**, 93–118.

NICOLL, R. S., LAURIE, J. R., SHERGOLD, J. H. & NIELSON, A. T. 1992. Preliminary correlation of latest Cambrian to Early Ordovician sea level events in Australia and Scandinavia. In *Global Perspectives on Ordovician*

Geology (eds B. Webby and J. R. Laurie), pp. 381–94. Rotterdam: Balkema.

OPDYKE, N. D., KENT, D. V. & LOWRIE, W. 1973. Details of magnetic polarity transitions recorded in a high deposition rate deep-sea core. *Earth and Planetary Science Letters* **20**, 315–24.

RIPPERDAN, R. L. & KIRSCHVINK, J. L. 1992. Paleomagnetic results from the Cambrian–Ordovician boundary section at Black Mountain, Georgina Basin, western Queensland, Australia. In *Global Perspectives on Ordovician Geology* (eds B. Webby and J. R. Laurie), pp. 93–103. Rotterdam; Balkema.

RIPPERDAN, R. L., MAGARITZ, M., NICOLL, R. S. & SHERGOLD, J. H. 1992. Simultaneous changes in carbon isotopes, sea level, and conodont biozones within the Cambrian–Ordovician boundary interval at Black Mountain, Australia. *Geology* **20**, 1039–42.

SCOTESE, C. R. 1987. Plate tectonic development of the Circum-Pacific (Panthallasic Ocean) during the Early Paleozic. In *Circum-Pacific Orogenic Belts and the Evolution of the Pacific Ocean Basin* (eds J. W. Monger and J. Francheteau), pp. 49–57. American Geophysical Union Geodynamics Series no 18.

SHERGOLD, J. H. & NICOLL, R. S. 1992. Revised Cambrian–Ordovician boundary biostratigraphy, Black Mountain, western Queensland. In *Global Perspectives on Ordovician Geology* (eds B. Webby and J. R. Laurie), pp. 81–92. Rotterdam: Balkema.

WADLEIGH, M. A. & VEIZER, J. 1992. $^{18}O/^{16}O$ and $^{13}C/^{12}C$ in lower Paleozoic articulate brachiopods: Implications for the isotopic composition of seawater. *Geochimica et Cosmochimica Acta* **56**, 431–43.

ZACHOS, J. C. & ARTHUR, M. A. 1986. Paleoceanography of the Cretaceous/Tertiary boundary event; inferences from stable isotopic and other data. *Paleoceanography* **1**, 5–26.